SEARCH FOR HYPERVELOCITY STARS ONE PARSEC FROM THE GALACTIC CENTER

UCLA PHYSICS & ASTRONOMY REU 2008

CLAIRE DORMAN

ABSTRACT

The first hypervelocity stars, bodies with radial velocities greater than the escape speed of the Milky Way, have previously been observed only in the halo of our Galaxy. However, they are thought to originate near the Galactic center. We present the most extensive search to date for hypervelocity stars in this region. Our images were taken over a one year baseline with the W. M. Keck II 10 m telescope using laser guide star adaptive optics techniques to achieve diffraction-limited resolution in this very crowded field. Two candidates appear to be unbound to the Galactic center; to confirm their velocities, we will need to verify that they reside at the Galactic center, about 8 kpc from Earth. In addition, our analysis revealed that the optical distortion of our camera, OSIRIS, changed significantly between 2007 and 2008. We were able to correct for this effect for the purposes of this project, but would like to trace the distortion over a longer period of time in order to determine whether the change was due to a one-time disturbance or whether the OSIRIS distortion continuously changes with time.

1. INTRODUCTION

Twenty years ago, Hills et al predicted that, were, a black hole to exist at the center of the Milky, Way, it could lend enough energy to ordinary stars to eject them out of the galaxy at speeds greater than the escape velocity (Brown et al 2005). The confirmation of a central black hole, Sgr A*, in 1998 (Ghez et al 1998) strengthened the possibility of finding such stars, but it was not until 2005 that Warren Brown serendipitously discovered the first hypervelocity star in the Milky Way halo (Brown et al 2005). Since then, nine more unbound stars have been discovered, most of them by accident and all in the halo, far from their suspected origin.

The Hills mechanism, now the most widely accepted, suggests that hypervelocity stars originate as members of binaries that encounter a black hole. If one member of the binary becomes bound to the black hole, enough energy can be transferred to the other member to eject it radially outwards at very high speed. If the velocity exceeds the escape velocity of the Galaxy, then the star can be classified as "hypervelocity" (Brown et al 2005).

This ejection mechanism does not produce an abundance of speeding bodies; calculations indicate that it should eject only one star every hundred thousand years (Yu and Tremaine 2003). This calculation considers only the 8% of binaries that the authors deem most likely to participate in such breakup: solar mass stars separated by semimajor axes between 0.01 and 0.3 AU. The accuracy of this assumption is not critical, as these quantities contribute only weakly to the ejection rate.

Many variants on this mechanism can be found, among them interaction of a single star with a binary black hole and single-star encounters. However, these mechanisms are expected to eject stars infrequently, on the order of one every ten billion years (Yu and Tremaine 2003).

Date: October 2008.

While the leading theories differ on the details of ejection, they all agree that hypervelocity stars are created at the Galactic Center, home of Sgr A*. We would expect, then, to see a few such stars near the center of the Galaxy, soon after their ejection. Earlier this year, the Ghez group at UCLA performed the only search to date in this region, using images from the camera NIRC2 to calculate velocities. They did not find any stars with 2D radial velocities sufficient to escape the Galaxy. This paper details a second search, in a field slightly farther from the Galactic center, using images from a different instrument.

2. DATA

Our strategy was to find the proper motions of stars near the Galactic center, and to compare each velocity to the escape velocity of the Milky Way evaluated at the star's position. To find the velocities, we used images of the Galactic center taken in 2007 and in 2008 and used astrometric techniques to accurately find the displacement of each light source over the ten month span.

All images were taken with the W.M. Keck II Telescope using the new camera OSIRIS, which uses Laser Guide Star Adaptive Optics techniques to eliminate atmospheric turbulence effects and achieve diffraction-limited resolution. Each set consisted of ten images, each in turn a superposition of ten two-second coadds from the Kn3 band. Our primary science images were taken on 19 July 2007 and 16 May 2008. Skies and flats were taken with the same setup but on different nights: in 2007, the skies were taken on the 17th of July and flats on 17 May. 2008's flats were taken on the 8th of June, and skies on the 16th of May. As the skies and flats are only used for normalization purposes, we did not expect this to have any effect on the measured positions of stars.

In contrast to the field searched earlier this year, ours was not centered on Sgr A*; its center was about 0.8 pc away. This is due to the fact that OSIRIS has both a spectrometer and an imager, offset from each other by 27.5 degrees and about 1 pc. On the nights we took our pictures, the spectrometer was aimed at the Galactic Center and so the imager was offset, as shown in the diagram below. We used OSIRIS' 20 mas plate scale, so that the 1024 × 1024 search area spans 20 by 20 arcseconds (shown as the light blue area in Figure 1).
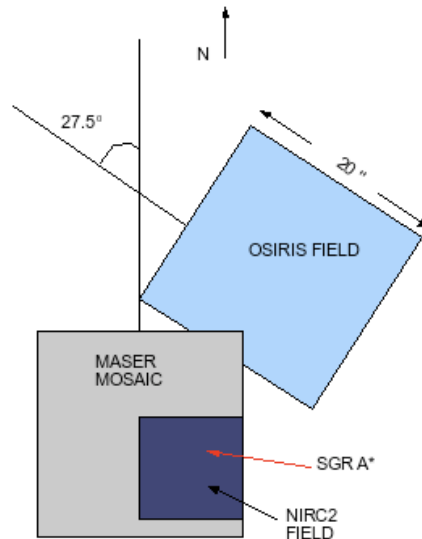
Figure 1. This figure shows the relative locations, orientations, and sizes of three fields. NIRC2's traditional field, centered on Sgr A*, spans 10″ by 10.″ The maser mosaic is the 20 by 20 ″ mosaic of NIRC2 images that our group searched for hypervelocity stars earlier this year. Both fields are oriented at a PA of 0 relative to north up. OSIRIS has a 20″ by 20″ field, located between 0.4 and 1.3 pc from Sgr A*, and is rotated at a PA of -27.5 degrees.

We wrote a new data reduction pipeline for OSIRIS images, as all previous reduction had been done only on NIRC2. This pipeline works in the standard way, creating for each epoch the standard main map and three submaps for rms error calculation. We used a centroiding program called Starfinder to create a PSF from a bright, isolated star in each main map. By successive iteration, Starfinder identified acceptable point sources in each of the 4 maps for its epoch. A star in a submap was considered acceptable if its correlation coefficient with the PSF was at least 0.6; a star in the main map needed a correlation of at least 0.8.

Next we aligned the maps within each epoch, allowing the coordinate systems of each submap to stretch in the x and y directions as well as rotate in order to best align with the main map and determine which stars in a main map were also present in a submap. A star was considered "confirmed" in an epoch if it appeared in both the main map and two of the three submaps. We also aligned the main maps of the two epochs, this time also allowing the pixel sizes of the images to adjust for a best fit. In the end, 1706 confirmed stars were present in both 2007 and in 2008. These constituted our sample. The mean rms position error was 1.28 mas and the corresponding velocity error 2.27 mas/yr. We did not calibrate magnitudes because it was unnecessary for our purposes.

Epoch	2007	2008
Image Date	19 July	16 May 2008
Image Set Number	34	32
Sky Date	20 July	17 May
Sky set number	24	38
Flat Date	17 May	03 June
Flat set number on, off	12, 11	13, 12
Filter	Kn3	Kn3
Integration Time	2 sec	2 sec
Coadds	10	10
Number of Images	8	10
FWHM from Gaussian fit to PSF (x, y)	2.4, 2.6	2.7, 3.7
Number of confirmed stars	2859	1762
Saturation Level	Significant	Not noticeable by eye

Table 1 summarizes the properties of the data sets we used. All images were taken with the same setup and reduced using the same process (with the exception that we had only 8 science images from 2007, two fewer than from 2008). The most significant difference is the relatively low quality of the 2007 images. Their psf is much more elongated than the 2008 psf, and the saturation level much higher. While more stars were confirmed from 2007, none of the 10 brightest stars in the region made it into this set, the most likely reason being saturation. As a result, none of the brightest stars were included in our study.

3. Data Analysis

We chose to eliminate all stars with fairly large positional uncertainties. Figure 2 shows the relative magnitude plotted against positional uncertainty. In an effort to keep only those stars for which we had precise position measurements, we cut all sources fainter than magnitude 13 on our relative scale (we did not calibrate magnitudes). At this point, all positional errors lay within 2 σ

of the mean, so we took no further position-error cuts. This left 906 stars among which to search for hypervelocity candidates.
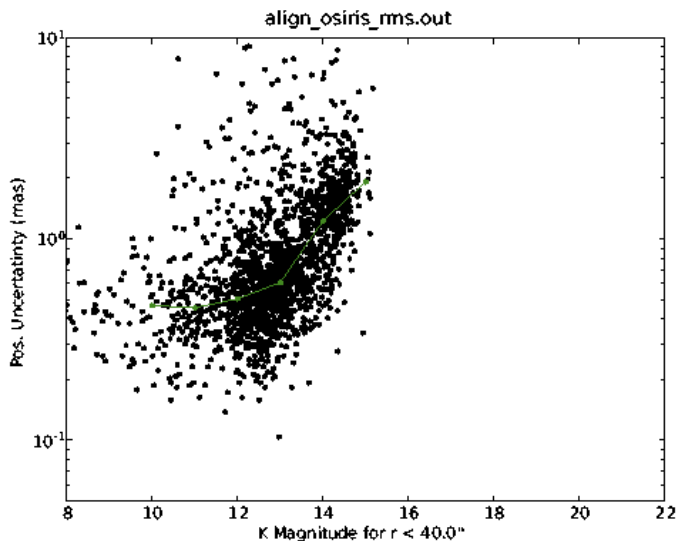
Figure 2 shows the relative magnitude of our sample of 1706 stars plotted vs. positional uncertainty as calculated by StarFinder. It is clear that for stars fainter than relative magnitude 13, the uncertainty is a rapidly increasing function of magnitude. Note that we did not calibrate our magnitudes, and so our cut should be interpreted simply as a cut of the 800 faintest stars.

3.1. **Unexpected Sysematics.** A plot of the velocity vectors of these 906 stars reveals unexpected systematics. One would expect the directions of proper motions to be randomly distributed, but both the upper and lower left corners of figure 3a (top) show significant directed flow on a scale of about 200 pixels (1/25th of the image size). In an attempt to characterize the flow distribution, we divided the field into twenty-five identically sized regions and calculated the mean velocity in each region. The results are plotted in figure 3b (bottom left). The deviation from 0, the expected average, ranges from 100 to 300 km/s, which is the same order of magnitude as our rms velocity error. The significance, however, lies in the distribution of anomalies. Compare figure 3b to 3c, which shows the classic "pincushion" optical distortion commonly seen in imager plates whose distortion patterns change over time.

4
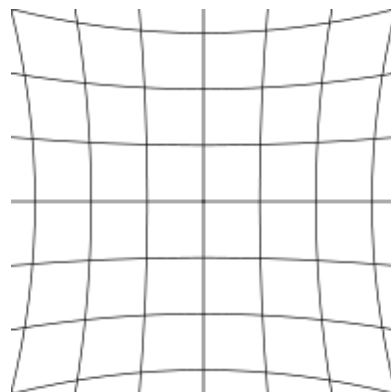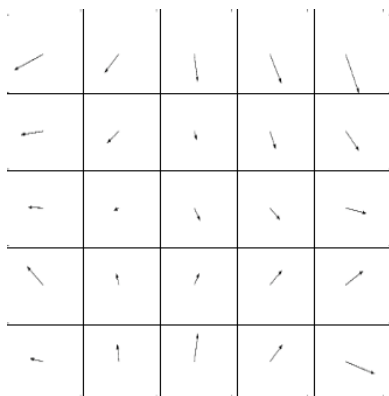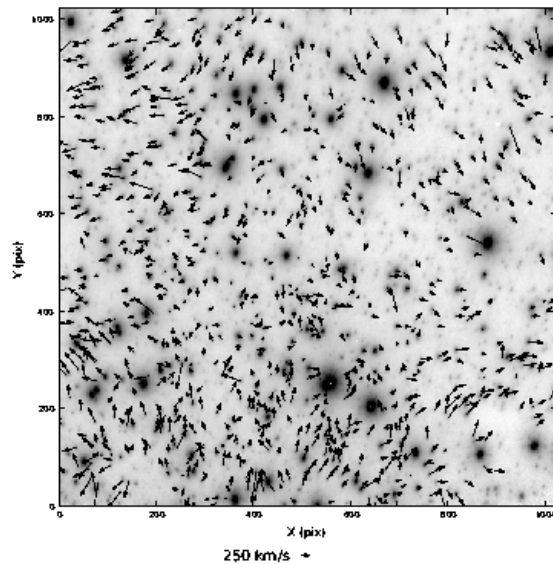
Figure 3. In Figure 3a (top), the systematics in the velocity directions are compelling evidence for distortion change between 2007 and 2008. Figures 3b (bottom left) depicts the average velocity in each of 25 equally sized bins. The deviation from zero in each bin, shown in figure 3c, is a rough map of the pattern of distortion change of OSIRIS between July 2007 and May 2008. The longest arrows represent a velocity of about 300 km/s. This distortion change appears to be symmetric: smallest in the middle and most pronounced near each of the four corners. This tendency mirrors that of an optical system subject to "pincushion" distortion, a schematic of which is shown on the right.

Something, then, must have caused a change in the distortion of OSIRIS in the ten months between July 2007 and May 2008. The most likely cause is the service run to the OSIRIS spectrometer in March 2008. While the service run was not intended to adjust the imager in any way, the disturbance to the camera may have been enough to produce the observed pincushion pattern.

Regardless of the cause of the distortion change, we could not proceed to measure velocities when their projections onto our image plane were affected in this way. We used the following method to account for this distortion. The average velocity in each of the 25 regions should, in an undistorted system, have been zero. By subtracting the average velocity (as shown in figure 3b) from each velocity vector in the respective region, we forced the mean velocity in each bin to

be zero. The resulting velocity distribution is showing in figure 3c. Notice how the vectors are significantly randomized compared to 3a, but still has some flow, especially along the left edge and in the lower left corner. We decided to ignore all sources within 75 pixels of the lower edge, and in the 100 by 100 pixel corner in the lower left.
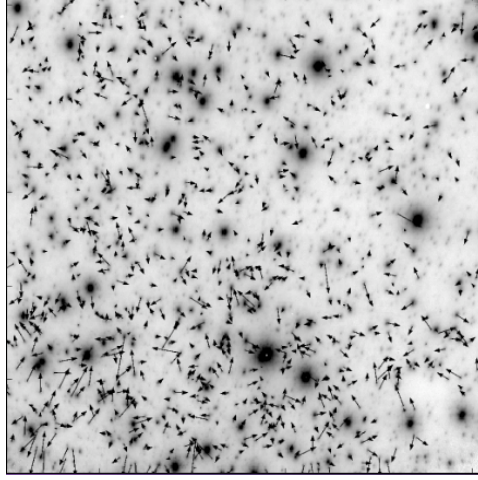
FIgure 4, 1024 x 1024 pixels. To account for the apparent change in optical distortion, we subtracted from each velocity the mean value of the velocities of all neighboring stars. In essence, this amounts to subtracting figure 3b from 3a. The result, shown in figure 4, is a randomized velocity distribution. Note that stars who appeared to be moving in the same direction as their neighbors were slowed down by our adjustment, while stars already moving in opposite directions now appear to be moving even faster than before. The correction tended to exacerbate the already marked downward flow on the bottom edge of the field, and so we did not include these stars in any further analysis.

3.2. **Gravitational Potential.** To decide which stars were unbound to the black hole, we compared the velocities to the escape velocity caused by a point mass of 4.2 solar masses which is the Ghez group value for the mass of the black hole:

$$v_{esc} = \sqrt{\frac{2GM_{encl}}{R}} = \sqrt{\frac{2G(4.42 \times 10^6 M_\odot)}{R}}$$

We considered as candidates the six stars with velocities more than 3 σ above the escape velocity curve. These stars are shown in figure 5.

However, since the middle of the OSIRIS field is a full parsec away from the Galactic Center, this formula is incomplete. Mass other than the black hole might contribute a significant amount to the gravitational potential. To examine this effect, we used a mass function presented by Schodel et al (2007), which describes a distribution dominated by the mass of the black hole up to a critical radius R_b, and then increasing almost linearly for the next several parsecs. The regions internal and external to R_b, the "cusp" and "cluster," respectively, are characterized by dimensionless parameters Γ_c and Γ_{CL}. This structure implies that there are two separate expressions for the enclosed mass, depending on whether the radius of interest is less than or greater than R_b. However, R_b is only 0.22 pc, about half the distance of the nearest star in our field, and so we only evaluated the mass for the region external to the break radius. The final expression for the escape velocity is given by:

$$v_{esc} = \sqrt{\frac{2GM_{encl}}{r}}$$
$$= \sqrt{\frac{2G}{r}} \sqrt{\frac{R_b^3(3 - \Gamma_{CL}) + [r^{3-\Gamma_{CL}}(R_b^{\Gamma_{CL}} - R_b^3)](2 - \Gamma_c)(2 - \Gamma_{CL})}{(3 - \Gamma_c)(3 - \Gamma_{CL})[R_b^2(2 - \Gamma_{CL}) + (R_b^{\Gamma_{CL}}r^{2-\Gamma_{CL}} - R_b^2)(2 - \Gamma_c)]} + M_{extra}}$$

6

where all the constants and uncertainties are given in Table 2. The mass distribution is graphed as a function of radius in figure 5b. It is mostly linear in the region of interest, although its uncertainty increases significantly at large distance from Sgr A*. At the farthest corner of the field, the escape velocity for the mass distribution is over two hundred km/s greater than the escape velocity calculated for the point source potential. In this new model, the number of stars with velocities more than 3σ above the escape velocity of the Galactic center decreased to two. We now turn our attention to these candidates.

R_b	0.22 ± 0.04 pc
σ_z	100.9 ± 7.7 km/s
Γ_c	0.19 ± 0.05
Γ_{CL}	0.75 ± 0.10
M_{extra}	$0.82 \times 10^6 M_\odot$
r	distance from Sgr A*

Table 2. These are the parameters we used to calculate the escape velocity in the vicinity of the black hole. All parameters are as given by Schodel (2007) except for the mass of the black hole (for which we used the Ghez value) and, of course, the distance of each star from Sgr A.*
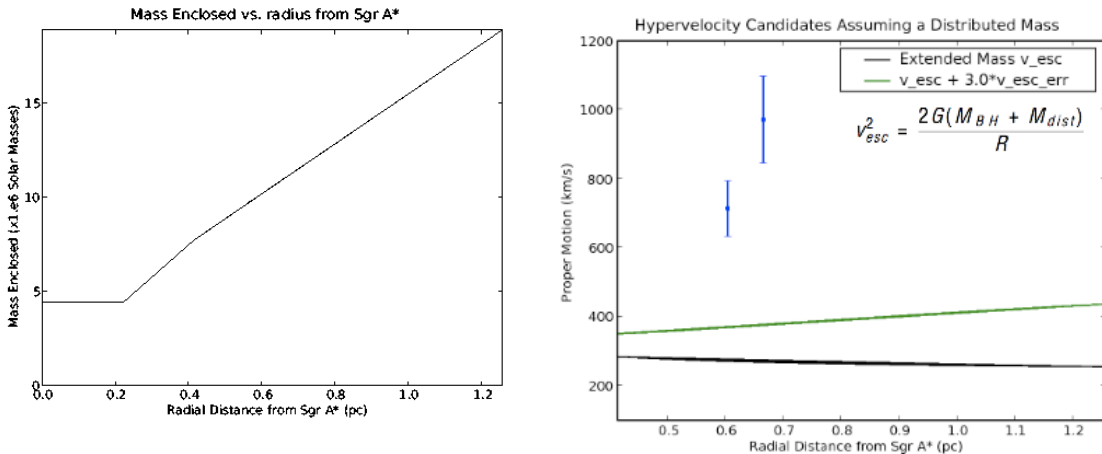
Figure 5. The mass distribution function in the region $r > 0.22$pc receives substantial contribution from bodies other than the black hole. The total mass gives rise to an escape velocity that is nearly linear in the region of interest, as opposed to the $\frac{1}{\sqrt{r}}$ dependence of the point source potential. The green line represents $v_{esc} + 3\sigma v_{esc}$, and it increases with radius because the uncertainty in r increases with radius. The two candidates with velocities more than 3σ above the green line are shown in blue.

4. RESULTS AND DISCUSSION

Both candidates reside in the lower left corner of the field, closest to the Galactic Center and also closest to the center of greatest remaining distortion. The radial velocity of those labeled 395 (red) and 197 (green) are, respectively, 657 ± 80 km/s and 950 ± 175 km/s. The escape velocity of the Milky Way at this radius is less than half of this, 270 ± 35 km/s. The tangential velocities within 2σ of zero. These observations are consistent with the theory that hypervelocity stars are ejected from

the Galactic center and travel on a radial trajectory. However, candidate 395 is traveling towards the black hole that, in theory, ejected it.
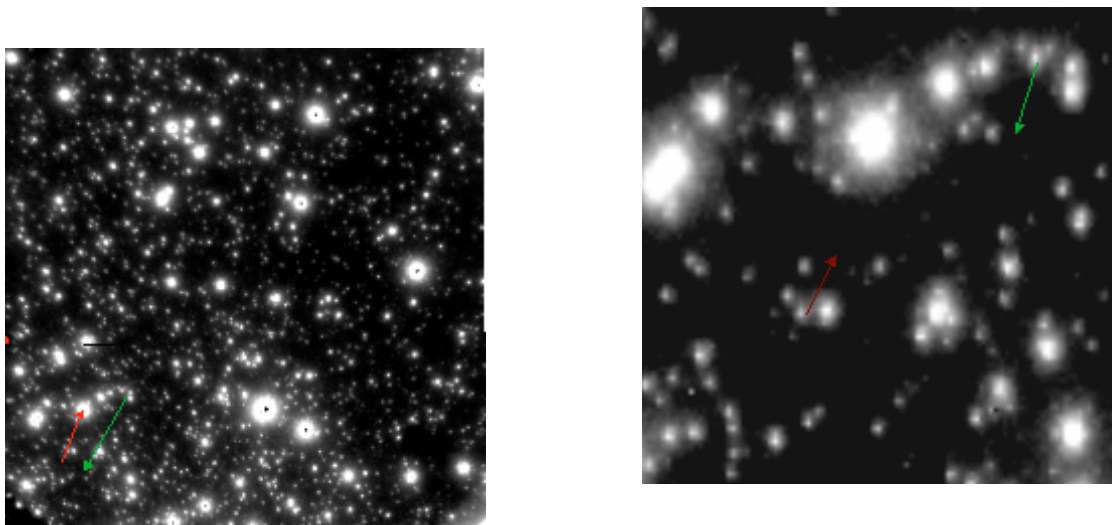
Figure 6. 6a (left) shows that both the candidates are located in the lower left quadrant of the field, where the remaining distortion was highest. 6b, a 250 x 250 pixel cutout of the lower left of the field, shows that the stars are separated by roughly 250 pixels and are moving away from each other. One of the stars is moving, within 2σ, away from Sgr A*, while the other is moving towards the black hole.

If these stars are indeed hypervelocity, their spatial density is much greater than predicted by Yu and Tremaine's analysis. The comparison is difficult since their conclusion is that stars are ejected isotropically at a rate of $10^{-5}yr^{-1}$, and our field is just a plane extending from 0.4 to 1.3 pc from the Galactic center. Assuming as an extreme upper limit to the expected density that every star ejected passed through our plane of observation, our observed density is 400 times greater than that predicted by Yu and Tremaine. In reality, with spherically symmetric ejection, the dichotomy between findings and predictions is even more extreme.

There are a couple of ways to account for the inward trajectory and the high density. In regards to the inwards-traveling star, it is possible that it was ejected from the center long ago, but slowed down so much on its way out of the Galaxy that it turned around and headed back towards where it came from, as if it were attached to the end of a spring that oscillates about the center of the Galaxy. This would mean that the star is unbound to the Galactic center but bound to the Galaxy. By using existing mass distribution functions, we hope to calculate how far away this star must have been when it turned around in order to have its present velocity.

It is also possible that the stars are not moving as quickly as we think. Both stars are in the lower left quadrant of the field, the part subject to the greatest distortion even after correction, and so their calculated velocities could be dramatically inaccurate. They were both hypervelocity candidates moving against the directed flow of a nearby region before correction, and the correction actually increased their apparent speeds. Were we to divide the field in another way, these stars might fall into a different correction region and subtracting the average velocity might decrease the speed. Finally, one or both of these stars could be foreground stars for which 1 mas does not translate to half a billion kilometers. To find their true linear speeds, we will need to confirm their distances using spectroscopy.

In addition to finding potential hypervelocity stars, this study revealed that the optical distortion of OSIRIS changed dramatically between 2007 and 2008. While this may be an unintentional

consequence of the March 2008 service run, other possibilities remain open. We would like to compare image sets taken entirely after the March mission and see if the distortion appears constant. Either way, it would be helpful to quantify the distortion change so that images taken before and after the change can be more precisely corrected.

5. Summary

We compared the velocities of 906 stars near the Galactic center to the escape velocity of the Milky Way, accounting for contributions of a mass distribution to the gravitational potential. We found two candidates which appear to be unbound to the Galactic center. One of them appears to be moving away from the black hole, as would be expected had it been ejected by Hills' mechanism. The apparent trajectory of the other, however, points radially inward. More work will need to be done before we can say whether either of these are indeed hypervelocity stars, especially since the affirmative would call into question the extremely slow ejection rate of the Hills ejection mechanism. In addition, we found that the optical distortion of OSIRIS changed over time in accordance with the classic "pincushion" pattern, and we are interested in quantifying the extent of the distortion over a longer period of time.

6. Acknowledgements

7. References

Brown, W., Geller, M., Kenyon, S., & Kurtz, M. 2005, ApJ, 622, L33
Ghez, A. M., et al. 1998, ApJ, 509, 678
Schodel, R., et al. 2007, A & A 469, 125146
Yu, Q., and Tremaine, S. 2003, ApJ, 599, 1129